INTERNATIONAL JOURNAL OF HYDROGEN ENERGY 39 (2014) 4981–4995

Available online at www.sciencedirect.com

ScienceDirect

journal homepage: www.elsevier.com/locate/he

Defect engineering of graphene for effective hydrogen storage

*Shwetank Yadav, Zhihui Zhu, Chandra Veer Singh**

Department of Materials Science and Engineering, University of Toronto, 184 College Street, Suite 140, Toronto, Ontario M5S 3E4, Canada

ARTICLE INFO

Article history:
Received 12 November 2013
Received in revised form
7 January 2014
Accepted 10 January 2014
Available online 13 February 2014

Keywords:
Hydrogen storage
Graphene
Topological defects
Defect-engineering
Physisorption

ABSTRACT

Although several modifications to graphene have been proposed to improve its hydrogen binding to practical levels, current theoretical studies largely neglect the role of topological defects. In this paper we analyze the effect of these defects and their possible use in a hydrogen storage system. Hydrogen physisorption on five types of point defects (Stone-Wales, single vacancy and three types of double vacancy) was investigated using density functional theory with the PBE-GGA functional. Point defects were also repeated with the vdW-DF2 functional to better represent long range van der Waals interactions. Although none of the defects were found to be detrimental to hydrogen anchoring, only the single vacancy showed promising hydrogen binding in the ideal range. Model systems combining different defects were also explored, including a defect-anchored metal system, a bilayer graphene system and a grain-boundary system. Finally, two high defect density structures constructed using vacancies and combined Stone-Wales defects and vacancies yielded gravimetric densities of 5.81% and 7.02%, respectively, with the vdW functional. This study suggests that graphene can be defect-engineered to develop effective hydrogen storage media.

1. Introduction

Hydrogen is considered to be a promising environmentally friendly fuel for the future as it possesses a very high energy content by mass compared to conventional fuels and can cleanly produce energy with no harmful by-products. However, it is impractical to store and transport hydrogen using existing methods. Therefore, research efforts in recent years have focused on finding systems which can store hydrogen through adsorption on various media [1], with an initial goal of 5.5 wt% gravimetric capacity targeted by the US Department of Energy (DOE) [2]. A class of materials that can act as effective adsorption media for hydrogen molecules are carbon-based nanostructures, due to their relative low weight and high surface areas [3,4]. Amongst these, graphene is considered particularly promising as a one atom thick two-dimensional structure gives it the highest specific surface area among these materials [5].

The need for reversible storage, where hydrogen can be both easily stored and released under near-ambient conditions, requires that hydrogen binding should be neither too strong nor too weak. Based on this practical need, the ideal binding energy range for reversible hydrogen adsorption is considered to be between −0.2 and −0.6 eV [6]. Pristine graphene, with a hydrogen binding energy in the range

* *Corresponding author*. Tel.: +1 (416) 946 5211; fax: +1 (416) 978 4155.
E-mail address: chandraveer.singh@utoronto.ca (C.V. Singh).

0360-3199/$ – see front matter
http://dx.doi.org/10.1016/j.ijhydene.2014.01.051

of −0.01 to −0.09 eV, does not meet this requirement [7,8]. Consequently, several modifications to graphene have been proposed to improve its storage capacity. They include metal decoration [9,10], doping with hetero-atoms such as nitrogen and oxygen [11,12], and the introduction of strain, curvature and edges [8]. An important issue with these studies is that they analyze idealized graphene structures and usually ignore the effect of defects on hydrogen adsorption, even though commercially prepared graphene sheets would typically contain topological defects [13]. When they are considered in some studies, defects are looked at for the sole purpose of anchoring metal atoms over defect sites [14]. To the best of our knowledge, the direct interaction of defects with hydrogen molecules and their modifying role in hydrogen adsorption has not been characterized thus far in the literature.

Furthermore, the metal-decorated systems studied so far have not been reproduced experimentally, rendering these theoretical results less useful in practice. There are additional concerns to these proposed systems. For instance, metal-decorated systems require the challenging task of isolating and placing single metal atoms at exact locations over the graphene layer, which might prove difficult to achieve under experimental conditions. On the other hand, the creation and control of topological defects over graphene layers has already been demonstrated experimentally [15]. Importantly, defect control would still be required for many proposed metal-decorated systems. Thus, it is necessary to understand the fundamental role of defects in graphene with respect to its hydrogen storage ability. Moreover, if defective graphene is shown to have sufficient binding ability, a system modified solely with defects would be potentially easier to implement in practice than the current proposed approaches.

In this paper, the hydrogen molecule binding ability of a graphene sheet with the Stone-Wales (SW), single vacancy (SV) and double vacancy (DV) 585, 555-777 and 5555-6-7777 defects is investigated. These five point defects were chosen as they have been observed experimentally and are known to be stable at room temperature. They are usually formed during manufacturing processes such as chemical vapor deposition, or can be induced by irradiation with electrons or ions [13]. The hydrogen binding ability in each case was evaluated using density functional theory (DFT) with the generalized gradient approximation (GGA) functional. The GGA functional is good at modeling covalent type bonding but poorly represents van der Waals (vdW) forces. Although vdW forces are negligible in covalent bonding dominated systems, they are a significant component in hydrogen molecule adsorption. Hence, all systems were also studied with the recently implemented vdW-DF2 functional [16] which better accounts for vdW forces. The consideration of vdW interactions usually resulted in higher hydrogen binding energies.

Based on the individual defect simulation results, a combined SW and SV defect system was created to investigate mixed defect regions. Similarly, a system consisting of SV anchored metal atoms with adjacent undecorated SVs was created to investigate the effect of undecorated vacancies on the hydrogen binding ability of metal atoms. A grain boundary structure, commonly created during graphene synthesis [13], was also investigated for hydrogen adsorption. Finally, the results of the individual and mixed defect simulations were utilized to engineer two high defect density structures to evaluate the maximum possible hydrogen molecule adsorption in graphene systems modified solely using defects. The first system consisted of closely spaced SVs, named the single vacancy maximum hydrogen density (SVMD) system. The second system consisted of half SW and half SV defects, named the Stone Wales single vacancy maximum hydrogen density (SWSVMD) system.

2. Computational details

The simulations were performed using plane wave based DFT as implemented in the Quantum Espresso software [17]. The exchange-correlation functional was represented using GGA as described by Perdew–Burke–Ernzerhof (PBE) [18]. Interactions between the valence electrons and the ionic core were represented by Vanderbilt Ultra-Soft Pseudopotentials [19]. The kinetic energy cutoff for wavefunction expansion was set at 60 Ry (1 Ry = 13.61 eV) and for the charge density it was set at 600 Ry. Each self consistent field calculation had a convergence threshold of 1E-5 Ry for the total system energy. Each system was relaxed with variable cell size using conjugate gradient minimization until the magnitude of the residual Hellman–Feynman force on each atom was less than 1E-3 Ry/Bohr. The total system energy during relaxation was minimized to within 1E-3 Ry. Brillouin zone integrations were performed using a Monkhorst-Pack grid with 8 × 8 × 1 k-points [20].

All simulations, except for the SVMD and SWSVMD systems, were performed with a vacuum spacing of 30 Å to sufficiently isolate the graphene layer and remove interactive effects between layers. All such simulations also allowed variable cell dimensions during system relaxation. The SVMD and SWSVMD systems were first simulated using a vacuum spacing of 6 Å and variable cell dimensions to allow for enhanced hydrogen adsorption through interaction effects between graphene layers. Subsequently, the effect of interlayer spacing effects was investigated for both SVMD and SWSVMD systems using fixed cell dimensions and vacuum spacings ranging from 2 to 7 Å. For the individual defect simulations, the graphene sheet size varied in proportion to the defect size so as to minimize interaction energies between periodic defect images. Specifically, the pristine graphene and SW supercells were modeled using 50 carbon atom 4 × 4 graphene sheets, while the SV used a 49 atom 4 × 4 sheet. The supercell containing the 585 DV was modeled using a 58 atom 4 × 5 sheet; the 555-777 DV using a 72 atom 5 × 5 sheet; and the 5555-6-7777 DV using a 82 atom 5 × 6 sheet. Bilayer graphene was modelled using a 24 atom sheet stacked with a 23 atom sheet in an AB stacking configuration. The mixed SV and SW system and the SWSVMD system were modeled using a 49 carbon atom 4 × 4 graphene sheet. The metal decorated system and SVMD system simulations used 30 atom 3 × 3 sheets. The semi-metallic nature of graphene was represented using Methfessel–Paxton [21] smearing with a degauss value of 0.01. The binding energy of a hydrogen molecule for each system was calculated as:

$$E_b = \left(E_{system+iH_2} - E_{system} - iE_{H_2}\right)/i \quad (1)$$

where $E_{system+iH_2}$ is the total energy of the modified graphene system with hydrogen adsorbed, E_{system} is the total energy of the modified graphene system without hydrogen, E_{H_2} is the total energy of the free H_2 molecule and i corresponds to the number of H_2 molecules. In order to accurately obtain energy changes, the three simulations required to produce values for the terms on the right hand side of the equation used the same supercell size and parameters. The hydrogen molecule was placed in several starting configurations for each individual defect system by varying its position laterally across the sheet. Its orientation with regards to the plane of the sheet (perpendicular or parallel) was also analyzed.

It was recognized that, the PBE-GGA functional is only good at accounting for localized effects and describing strong bonds, but is not good at describing long-range nonlocal effects such as vdW forces which have long decay tails. There have been several functionals proposed to help better model such weak interactions, and among them the vdW-DF approach provides a generalized truly nonlocal functional independent of system geometry [22]. The vdW-DF2 functional is a further improvement over the originally proposed vdW-DF functional [16], and provides better equilibrium separations, hydrogen bond lengths and more accurate vdW interactions at intermediate distances longer than equilibrium ones. More importantly, for our purpose at hand, when compared with several DFT functional approaches, the vdW-DF2 functional has been found to most closely match experimental data for adsorption of a hydrogen molecule on copper surfaces [23], as well as molecular adsorption on metal surfaces [24]. All individual defect simulations were repeated with van der Waals corrections to the PBE-GGA through the vdW-DF2 functional while keeping all other simulation parameters the same. This allowed for comparison with previous literature and investigation of the effect of different density functionals. The remaining simulations were all performed solely with the vdW-DF2 correction since it probably models complex hydrogen systems more accurately. All atomic and charge density visualizations were created using XCrySDen software [25].

3. Hydrogen binding over individual defect systems

In this section, the five individual defect simulation results are presented and their binding energy values are available in Table 1. It was found that the orientation of the hydrogen molecule with regards to the plane of the sheet (perpendicular or parallel) had a negligible impact on binding energies and so only the differences in energy at different locations over the defect are reported in the table. The corresponding plots of charge density variation around each defect are found in Fig. 2. According to Eq. (1), a negative binding energy indicates favorable conditions for hydrogen adsorption, with a more negative value indicating stronger binding.

3.1. *Pristine graphene*

To establish a baseline for binding energy results, in comparison to which modifications of graphene should offer an advantage, hydrogen adsorption over pristine graphene was studied first. Previous literature [26] has shown that the hollow position, as shown in Fig. 1(a), has the lowest adsorption energy with a binding value of −0.011 eV using the PBE-GGA functional and −0.054 eV using the vdW-WF functional (another functional used to better represent vdW forces). In the current paper, the hydrogen binding energy of pristine graphene layer was found to be −0.010 eV using PBE-GGA (consistent with literature value) and −0.062 eV with vdW-DF2 (slightly different from Ref. [26] due to a different functional used for vdW interactions). These values indicate a very weak binding of hydrogen on pristine graphene, far from the preferred −0.2 to −0.6 eV range, and demonstrates that pristine graphene cannot fulfill the requirements for a practical hydrogen storage medium.

Table 1 – Binding energies of a hydrogen molecule placed over individual topological defects in graphene. Multiple positions, shown in Fig. 1, were tested for each defect type. Both PBE-GGA and vdW-DF2 functionals were utilized to ascertain differences in binding energies due to choice of density functional. The vdW-DF2 results all demonstrated stronger binding and a smaller range of values among sites within a defect than the PBE-GGA results.

	Binding energy (eV)	
	PBE-GGA	vdW-DF2
Pristine	−0.0102	−0.0618
Stone-Wales (SW)		
Top	−0.0100	−0.0610
Hepta	0.0011	−0.0620
Penta	−0.0136	−0.0727
Single vacancy (SV)	−0.3282	−0.4020
Double vacancy (DV)		
585		
Octa	−0.0082	−0.0624
Penta	−0.0156	−0.0646
555-777		
Bridge57	−0.0080	−0.0592
Bridge77	−0.0091	−0.0571
Top	−0.0037	−0.0542
Hepta	−0.0020	−0.0655
Penta	−0.0051	−0.0678
5555-6-7777		
Hepta	0.0009	−0.0614
Hex	−0.0067	−0.0618
Penta	−0.0127	−0.0656

3.2. *Stone-Wales defect*

For the SW defect, the hydrogen molecule was placed over three positions as indicated in Fig. 1(b). For the top position, the PBE-GGA binding energy was found to be identical to that of the pristine graphene case and seemed to offer no additional advantage for hydrogen binding. The penta position, however, offered a small improvement while the hepta position was unfavorable with a positive binding energy. The nonexistent binding in the hepta position is likely due to the hydrogen molecule's increased distance from the surrounding carbon atoms, resulting in weaker covalent interactions as represented by PBE-GGA. The reason for the better penta

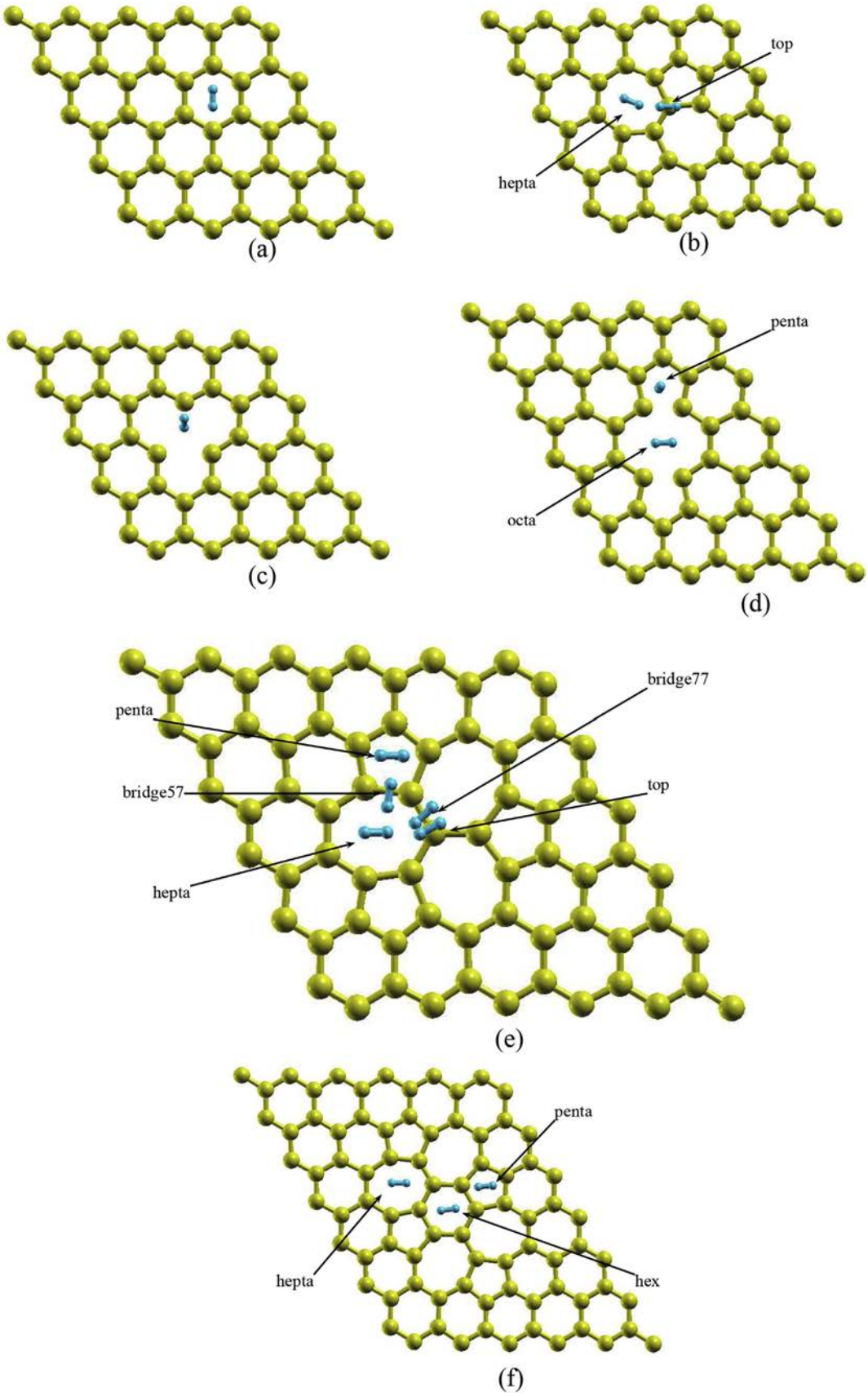

Fig. 1 – Supercells for hydrogen binding over individual defect systems depicting different initial positions for the adsorption of a hydrogen molecule: (a) Pristine (b) SW (c) SV (d) DV 585 (e) DV 555-777 (f) DV 5555-6-7777.

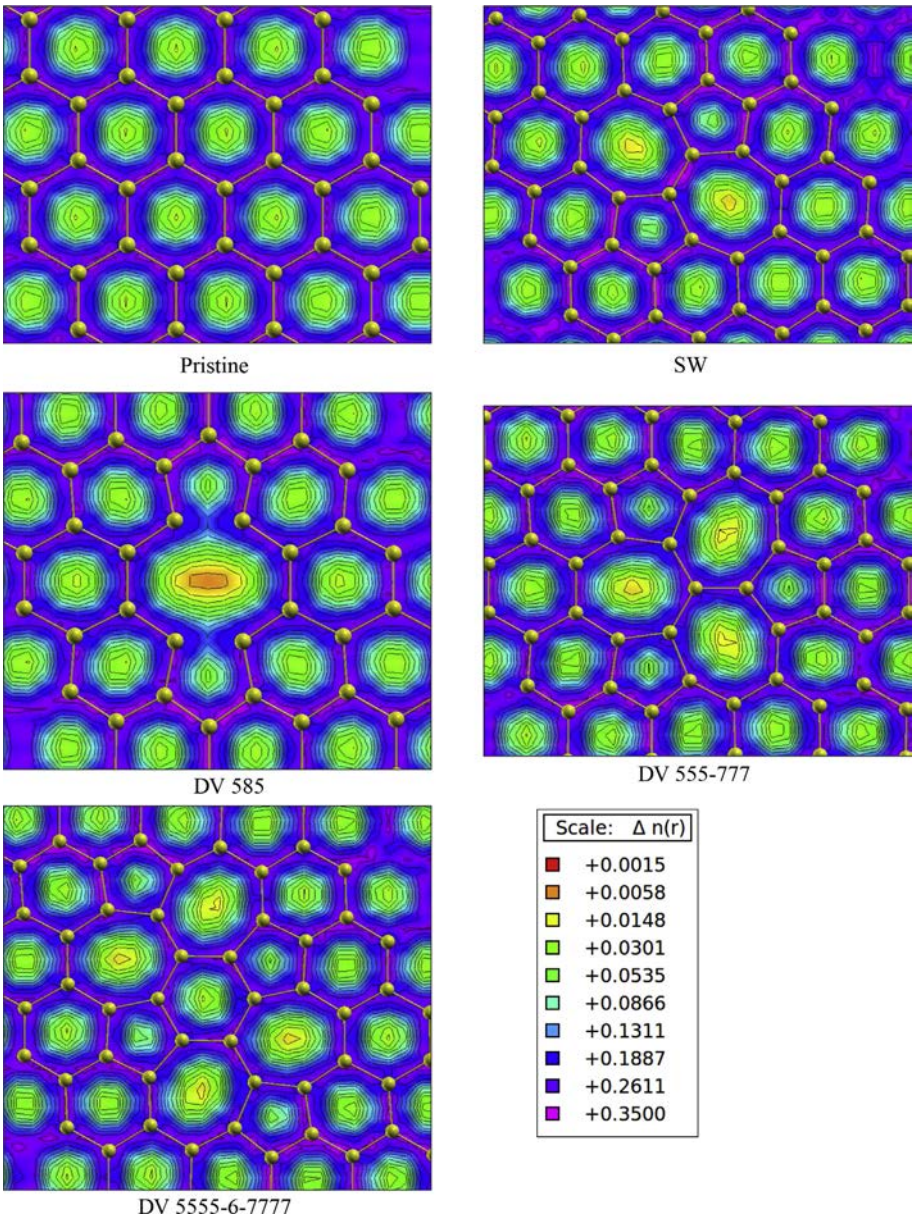

Fig. 2 – Top view of charge density for studied defective graphene systems except for SV, found in Fig. 8. The highest amount of charge can be seen to concentrate around the carbon atoms arranged in rings. Conversely, the lowest amount of charge is present in the hollow regions of these rings. The very high charge density around the carbon atoms make the top and bridge positions unfavourable for adsorption. Among hollow positions, the pentagon rings seem to have the most optimum charge density for favorable hydrogen adsorption, whereas the lower charge densities of the larger rings leads to slightly weaker binding energies.

binding energy was likely due to the closer equilibrium distance of the H_2 molecule to the surrounding ring atoms leading to a stronger interaction of the electrons in the hydrogen molecule with those of the carbon atoms. For the top position, there was a high density of electrons near the carbon atom, as shown in Fig. 2. This resulted in a relatively stronger repulsive force being felt by the hydrogen molecule, making this a less stable position.

For the vdW-DF2 calculations, the binding energy at top position was found to be very similar to that of pristine graphene. The hepta position was also found to have a virtually identical binding value, while the penta position offered slightly stronger binding. A previous study, using atomic orbital basis sets with GGA and Double Zeta Polarization (DBZ) for this system, has reported a binding value of −0.082 eV at the penta position and a binding value of −0.090 eV at the hepta position [27]. These are closest to the vdW-DF2 results in our study (−0.073 eV for penta and −0.0620 eV for hepta), suggesting the DBZ can provide corrections similar to those of vdW-DF2 for atomic basis sets, at least for this type of defect. These somewhat better values in the cited study could be due to differences in the DFT approach and simulation parameters, although in both cases the penta position is found to be slightly stronger than the hepta position. The stronger binding

energy of the hepta position for vdW-DF2 compared to PBE-GGA is likely due to vdW interactions which act over the increased distance of the hydrogen molecule from surrounding atoms. As can be seen, the SW binding values were still outside the preferred range of −0.2 to −0.6 eV. Yet, since the SW defect had a better binding ability than pristine graphene, it is expected that the presence of SW defects will increase the ability of a graphene system to draw hydrogen molecules closer to the surface even though it will not bind them strongly enough for practical purposes.

3.3. *Single vacancy defect*

The supercell for this defect system is shown in Fig. 1(c). The single vacancy defect was observed to have binding energy values much stronger than those for any of the other single layer individual defect systems. They fall comfortably within the desired range required for practical reversible adsorption. The vacancy has three carbon atoms adjacent to it, which were found to undergo significant movement after adsorption of the hydrogen molecule. This is quite different than the other studied individual defects, for which the carbon atoms did not undergo any appreciable movement after introduction of the hydrogen molecule. The change in the carbon atom configurations is shown in Fig. 3(a), a side cross-section of the graphene sheet prior to adsorption. From the figure, it is clear that the atoms were more or less contained within a single plane of the graphene sheet. However, after adsorption of the hydrogen molecule, as depicted in Fig. 3(b), the adjacent atoms have moved out of the plane of the sheet away from the hydrogen molecule. This configuration was found to be the most optimal in helping to share electronic charge between the hydrogen molecule and the atoms around the vacancy as further discussed in Section 5.

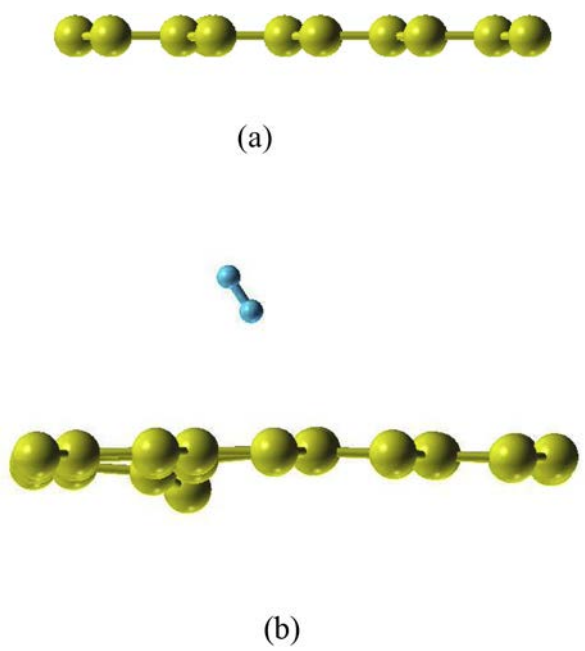

Fig. 3 – A side cross-section of the single vacancy defect: (a) prior to and (b) after adsorption of hydrogen molecule. Adsorption of the hydrogen molecule clearly distorts the graphene sheet, pushing the atoms adjacent to the vacancy out of the plane away from the hydrogen molecule.

A variable which might also affect hydrogen binding is the distance between defects in the graphene sheet. As the SV defect was found to be the most promising of the single layer individual defects, the effect of defect density was briefly investigated for this defect using different sized supercells. Both 31 carbon atom and 71 carbon atom supercells with an SV in each were simulated to observe the effect of higher and lower defect density respectively. The 31 atom supercell exhibited a hydrogen binding energy of −0.494 eV while the 71 atom supercell showed a hydrogen binding energy of −0.323 eV. This indicates a monotic increase in hydrogen binding strength with increasing defect density (created by decreasing supercell size) and was a motivation for creating the very high defect density structures studied in Sections 4.4 and 4.5.

3.4. *585 Double vacancy defect*

Two positions were investigated for the 585 defect for H_2 adsorption, as displayed in Fig. 1(d). While PBE-GGA showed large differences in binding energies between the two locations, with the penta position found to have the lower energy of the two, this positional difference was observed to be inconsequential in the case of the vdW-DF2 functional. This is similar to the case of the SW defect where the hepta (or octa here) position was at the center of a large region of very low electron density and far from the surrounding atoms, causing it to experience a lower amount of interaction with them (see Fig. 2). The use of vdW-DF2, on the other hand, allowed for interactions to occur over larger distances. The vdW-DF2 results displayed a much stronger binding of the hydrogen molecule than the PBE-GGA results, although they were only marginally better than the pristine graphene case and weaker than the preferred range of values.

3.5. *555-777 Double vacancy defect*

The 555-777 defect had the most unique available positions for the adsorption of the hydrogen molecule, a total of five as shown in Fig. 1(e). For PBE-GGA simulations, the hepta position produced the weakest binding energy, followed by the top position, penta position and the two bridge positions. On the other hand, for vdW-DF2, the top position displayed the weakest binding energy, followed by the two bridge positions, the hepta position and then the penta position. The vdW-DF2 results followed expected trends, similar to those seen for the SW and 585 defects, where the top and bridge positions possessed weaker binding energies due to the repulsion felt by the hydrogen molecule from close proximity to high electron density (see Fig. 2). The hepta and penta positions in the hollow of the rings both exhibited better binding energies as the hydrogen molecule can easily fill a region previously devoid of charge and interact well with electrons belonging to the surrounding carbon atoms. Once again, the penta position demonstrated slightly stronger binding than the larger hepta position, indicating that the penta position is closest to an

optimal distance from the surrounding carbon atoms. For the PBE-GGA simulations, the strange order of binding energies was likely due to the poor ability of the functional to account for vdW forces. The distance of the H_2 molecule was greater from surrounding atoms in hollow positions in the center of rings and this produced low stability due to the absence of long-range interactions. This caused the penta and hepta positions to have weaker binding energies relative to other positions. In fact, PBE-GGA results for all positions in this defect demonstrated weaker binding energies than the pristine graphene case. The vdW-DF2 results were only marginally better than the pristine graphene case and still weaker than the preferred range of values. As was the case in other individual defect systems, the spread in the binding energy values for vdW-DF2 cases was observed to be much smaller than that for the PBE-GGA calculations.

3.6. 5555-6-7777 Double vacancy defect

As depicted in Fig. 1(f), three positions were analyzed as potential sites for H_2 adsorption for the 5555-6-7777 defect. Both PBE-GGA and vdW-DF2 showed the hepta position with the weakest binding energy and the penta position with the strongest binding, following the same trends as SW, 585 and 555-777 defects. The PBE-GGA hepta position binding energy was exceptionally weak and actually the lowest binding energy of the individual point defect simulations in this paper. Once again, the vdW-DF2 simulations had similar binding values for all locations while the PBE-GGA showed a much wider spread. Again the vdW-DF2 binding energies were found to be much stronger than the PBE-GGA values but still offered no significant improvement over the vdW-DF2 pristine graphene results and do not lie in the preferred range of values.

3.7. Bilayer graphene with single vacancy defect

During graphene manufacturing, a particular form of graphene produced is bilayer graphene which has a specific interlayer spacing. In an attempt to study the effect of defects on hydrogen adsorption in this structure, bilayer graphene in an AB stacking with a SV defect on one of the layers was simulated for two cases. In the first case, the hydrogen molecule was placed above the defect and between the two carbon layers and in the second case the hydrogen molecule was placed above the defect as well as the entire bilayer structure. For the first case, the hydrogen binding energy turned out to be 0.505 eV while the second case resulted in a hydrogen binding energy of −2.824 eV. The first case was clearly unfavourable for hydrogen adsorption. The second case had a very strong binding energy which was well outside the preferred range of values and thus would be impractical in creating a reversible storage process. Furthermore, the bilayer structures consist of two carbon layers in which only one of the layers participates in hydrogen adsorption on one of its surfaces. This is quite inefficient and drastically reduces hydrogen density of the overall system. Finally, a bilayer structure with AA stacking falls within the range of interlayer spacings investigated for the high defect density structures explored in Sections 4.4 and 4.5.

4. Hydrogen binding over multiple defect systems

4.1. Grain boundary

Large scale graphene sheets, such as those synthesized from chemical vapor deposition, are usually polycrystalline and contain one dimensional defects along grain boundaries. These defects are generally tilt boundaries and can be thought of as a line of individual point defects [13]. Several such defects consisting of arrangements of pentagons and heptagons, found to be the most thermodynamically stable among possible ring structures, have been previously simulated to obtain mechanical properties [28]. One such system, shown in Fig. 4 and analogous to the Σ7 grain boundary defect, was selected to simulate the hydrogen adsorption ability of grain boundaries in graphene. This defect is likely representative of other similar grain boundary defects which also consist of ring structures. Our previous simulations suggest that these structures would have hydrogen adsorption abilities similar to other ring structure defects such as double vacancies. This was confirmed as the resulting binding energy of −0.081 eV was barely stronger than that of graphene and the point defects (beating the SW penta position by just 0.008 eV) and similarly outside of the range of values preferred for reversible storage. Thus, it can be reasonably concluded that while grain boundaries are not detrimental to hydrogen adsorption ability in graphene sheets, they do not offer much benefit either.

4.2. Mixed Stone-Wales and single vacancy

Both the SW and SV defects were modeled in the same supercell to study the effect of mixed defect regions. They were placed in close proximity and only separated by a hexagon ring of carbon atoms, as shown in Fig. 5. The SW defect penta position was studied, as this position presented the strongest binding energy after that of the SV in all individual point defect simulations. The binding energy of

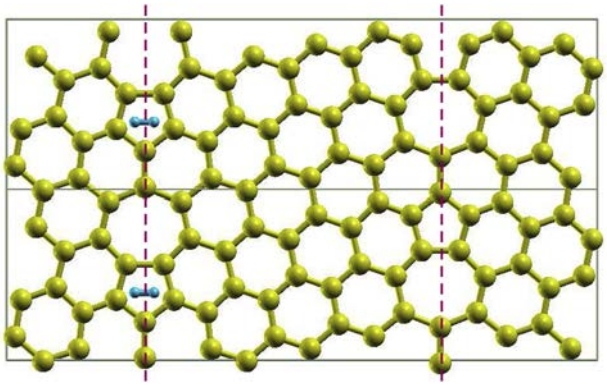

Fig. 4 – Grain boundary defect consisting of 5–7 rings, analogous to Σ7 defect, and adsorbed hydrogen molecules. Two adjacent supercells are shown to visualize the grain boundaries indicated by the dashed lines. Note the different orientations of the graphene lattice on each side of a grain boundary, indicating different grains.

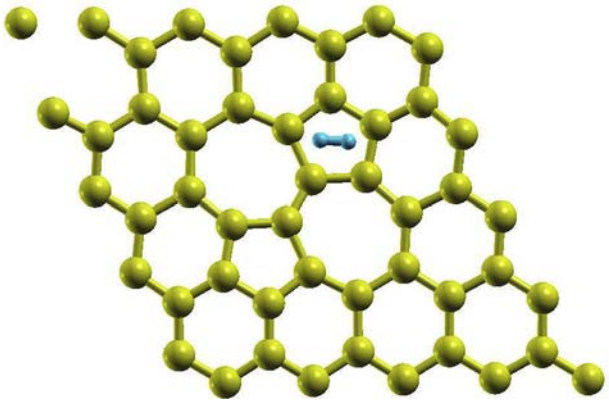

Fig. 5 – Mixed defect system showing single vacancy at the top-left and Stone-Wales in the center. The hydrogen molecule is adsorbed at the penta position in the Stone-Wales defect. The hydrogen binding energy is significantly higher in this mixed defect system than for either defect in isolation.

−0.545 eV at the penta position showed a significant improvement in binding ability, by a factor of 7.5 over the same position in the isolated SW defect, due to the presence of the single vacancy. This represents the highest H_2 binding energy amongst all 30 Å vacuum spacing single layer simulations. This system shows that the mixture of single vacancies with other point defects, unlike the mixture of only ring structure defects found in the grain boundary system, is very beneficial to hydrogen adsorption ability.

4.3. *Single vacancy with metal decoration*

A structure consisting of closely spaced SVs was modeled with double sided metal decoration. Only half the vacancies anchored nickel atoms as seen in Fig. 6, thereby ensuring each metal atom had an adjacent empty vacancy. The SVs themselves were separated from each other by at least a hexagon of carbon atoms. A hydrogen molecule was in turn adsorbed on each of the nickel atoms. The binding energy of −0.238 eV for each hydrogen molecule was found to be within the preferred range of values for practical hydrogen storage. However, it is lower than the value of −1.157 eV found for a similar system sans defects, simulated in a separate study by Wong et al. [29]. This suggests that the presence of adjacent SVs decreases the hydrogen binding ability of metal atoms. This is despite the fact that the metal atoms were anchored in vacancies, which in earlier studies have been shown to increase the hydrogen binding ability of metal atoms when there are no empty adjacent vacancies [30].

4.4. *Single vacancy maximum hydrogen density (SVMD) system*

A structure with a very high density of SVs, where the vacancies are separated by a minimum of only one hexagon of carbon atoms, was chosen to represent a defect engineered system for use in hydrogen storage as shown in Fig. 7(a). This structure was then packed with the maximum number of hydrogen molecules which were still able to produce a negative binding energy. In total 11 H_2 molecules were accommodated, which represents 5.81% gravimetric density for hydrogen storage. The change in the average H_2 binding energy with successive addition of molecules to the structure is shown in Fig. 9(a). The binding ability of the system rapidly drops after the first four hydrogen molecules, indicating that each vacancy is quickly stabilized and saturated by about two hydrogen molecules each. The lowest binding energy of −0.1 eV is just below the preferred range of values for reversible hydrogen storage. After relaxation, the interlayer spacing had decreased to 2.65 Å from the initial 6 Å. Nine of the hydrogen molecules had been split apart and their individual hydrogen atoms were observed to move closer to carbon atoms, as can be seen in Fig. 7(b). Most of these individual hydrogen atoms were now positioned over carbon atoms in the top position but stayed out of chemical bonding range. The exception was around the vacancy sites, where three hydrogen atoms appear to have moved into chemical

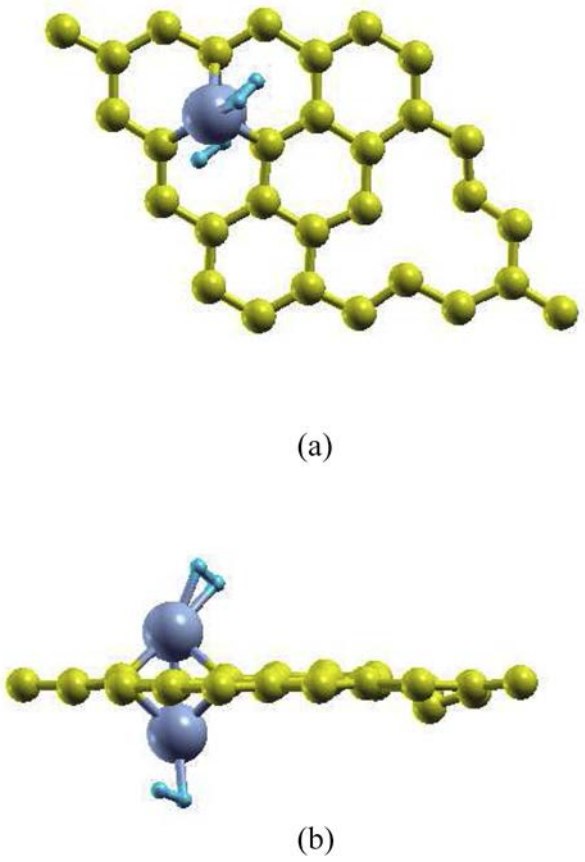

Fig. 6 – Single vacancy defect system with double-sided nickel metal decoration and hydrogen molecule adsorption: (a) top view and (b) side view. The nickel atoms are anchored over a single vacancy, while the adjacent vacancy is left undecorated. Although the hydrogen molecule binding energy is still within the preferred range for hydrogen storage, it is weaker than that of the corresponding system without vacancies.

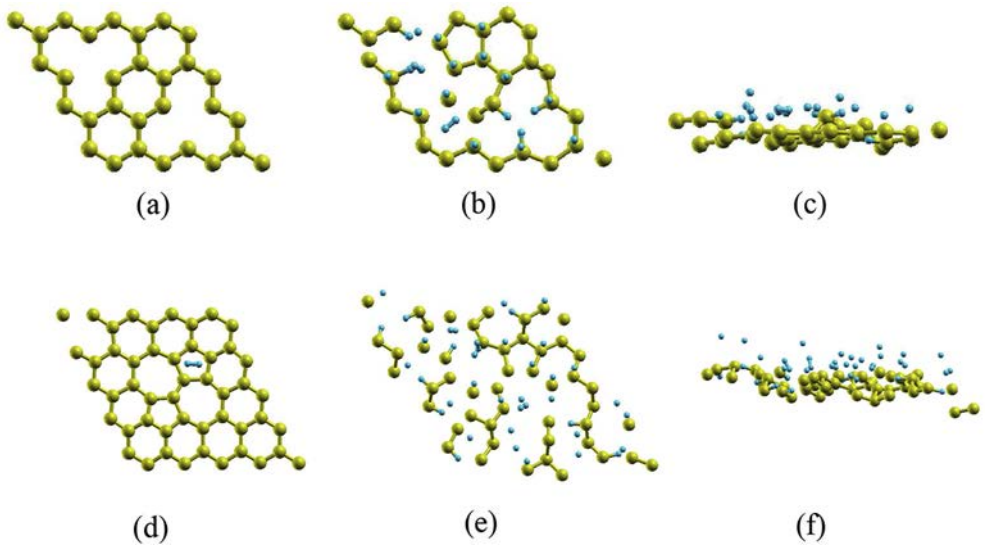

Fig. 7 – Defect engineered systems for hydrogen storage: (a) SVMD system prior to hydrogen adsorption, (b) SVMD system subsequent to hydrogen adsorption top view and (c) side view. A total of 11 hydrogen molecules were adsorbed to yield a gravimetric density of 5.81%. Nine of the hydrogen molecules dissociated into individual atoms. The underlying graphene sheet itself has undergone significant structural distortion subsequent to hydrogen adsorption. The SWSVMD system prior to adsorption (d) is also shown, and subsequent to hydrogen adsorption (b) top view and (c) side view.

bond range with the three carbon atoms surrounding each vacancy. The graphene structure itself underwent significant distortion from its flat planar shape as can be seen from Fig. 7(c). This suggests that the carbon and hydrogen atoms formed a complex network stable at the decreased interlayer spacing.

The effect of interlayer spacing was further explored by calculating the average hydrogen binding energy with different vacuum spacing in the supercell, going from 3 Å to 7 Å, the results of which are presented in Fig. 10(a). The strongest binding energy was found to be at 3 Å, a sharp drop from the energy at 2.65 Å which had been achieved when the supercell dimensions were allowed to vary during relaxation. There is also a sharp rise in energy when going to 4 Å, which displays an unstable positive average binding energy. Thereafter, the binding energy once again starts to decrease and become stable upto 7 Å, at which point it has even stronger than the energy at 2.65 Å.

4.5. *Stone Wales single vacancy maximum hydrogen density (SWSVMD) system*

The mixed SW and SV system investigated previously, seen in Fig. 7(d), was considered for use in a defect engineered hydrogen storage system in a manner similar to that of the SVMD system. In total, $22H_2$ molecules were successfully adsorbed, leading to 7.02% gravimetric density for hydrogen. The change in average H_2 binding energy with successive addition of molecules to the structure is shown in Fig. 9(b). The energy follows a more linear pattern than the SVMD system and displays fairly strong hydrogen binding. After relaxation, the interlayer spacing had decreased to 2.65 Å from the initial 6 Å, similar to the SVMD structure. Twenty of the hydrogen molecules had been dissociated and the substrate structure of carbon atoms itself was heavily distorted, as can be seen in Fig. 7(e). Several of the carbon rings, especially the heptagons in the SW defect, have broken up and carbon atoms have moved out of their standard sp^2 bond range to open up vacancy like gaps. Unlike the SVMD system, the individual hydrogen atoms did not seem to prefer the top position over carbon atoms and were more randomly distributed, with most not positioned directly over a carbon atom. The majority of hydrogen atoms were also well out of covalent bonding range of carbon atoms and positioned in the space between graphene layers, as seen in Fig. 7(f). Hence, the whole system consisting of carbon and hydrogen atoms appears to have rearranged itself to form a stable complex.

The effect of interlayer spacing was further explored by calculating the average hydrogen binding energy with different vacuum spacing in the supercell, going from 3 Å to 7 Å, the results of which are presented in Fig. 10(b). This range was selected as these provide a relatively practical range, with 3 Å being just below spacing for graphite and spacings beyond 7 Å reducing volumetric density. The strongest binding energy was found to be at 7 Å, while 3 Å provides the weakest binding energy.

5. Discussion: general trends towards defect engineering of graphene for hydrogen storage

In this section, we discuss the general trends in hydrogen binding over individual and mixed defect systems, identify important parameters which affect hydrogen adsorption ability and suggest a way towards defect-engineering of graphene for effective hydrogen storage.

5.1. *Individual defect systems*

5.1.1. *Choice of exchange functional*

The vdW-DF2 results consistently showed stronger binding values and a smaller range of these values among different sites within a defect than the PBE-GGA results. The adsorption of the hydrogen molecule itself appeared to be in the form of physisorption, which is typified by the molecule not dissociating and the lack of strong covalent character bonds between the hydrogen and carbon atoms. This kind of adsorption is dominated by weak interactive van der Waals forces. The vdW-DF2 functional captures such interactions much better than the plain PBE-GGA. Since van der Waals forces are mostly attractive except at very close range (at which point Pauli repulsion dominates), their inclusion generally results in a stronger binding of the hydrogen molecule to the graphene surface. Furthermore, since they act over a long-range, molecules experience similar levels of interactions regardless of their location in the studied ring structures. Conversely, the short-range covalent bond forming forces, modeled well by PBE-GGA, are highly localized and thus small changes in molecule position can cause large changes in the amount of interaction felt by the molecule and hence a larger variation in binding values for the same defect. As the vdW-DF2 results are more accurate for physisorbed systems, the following discussion summarizes key trends based on this functional's simulations.

5.1.2. *Ring structure defects*

The SV defect differs from other defective systems because all the other structures consist of convex polygon rings where the atoms have rearranged themselves to provide each carbon atom with bonds to three surrounding carbon atoms. On the other hand, the SV defect consists of a non-convex polygon in which atoms adjacent to the vacancy have bonds to only two other atoms. These differences lead to different hydrogen binding trends between the two types of defects. For non-SV structures, binding energy seems to be determined primarily by the distance of the hydrogen molecule from regions of charge. The highest electron density is found to concentrate around the carbon atoms arranged in rings, as can be seen from the top-view of charge density for each of the simulated systems (prior to hydrogen adsorption) in Fig. 2. These diagrams all display contours of charge density from 0.0015 to 0.35 (number of charge/Bohr^{-3}). The trends for binding energies in relation to the position of the hydrogen molecule on the defect can be qualitatively understood by carefully analyzing these contours. It can be observed that top and bridge positions over regions of very high charge have weak binding ability, likely due to the appreciable Pauli repulsion felt by the hydrogen molecule. This is in fact opposite to the case of chemisorption of a single hydrogen atom over graphene, where the top position would be most preferable as it helps stabilize the charge deficient atom [31].

For ring structures (ranging in size from pentagons to octagons), the charge density is observed to decrease towards the center of the ring. This suggests that hydrogen binding improves in going from hollow positions in octagons to heptagons to hexagons and finally pentagons, with the last position showing the most optimal distance from surrounding charge among ring structures. These binding energy trends hold true within the same defect for different hydrogen molecule positions, but not across different defect types. For instance, the octagon ring in the DV 585 defect displayed a weaker binding energy than the pentagon ring in the same defect as expected, yet it showed a stronger binding energy than the hexagonal and heptagonal positions in the DV 5555-6-7777 defect and in pristine graphene. This could be due to the different sizes of the same type of ring found in different defects and also due to the nature of the surrounding rings. Each ring is somewhat distorted from its regular geometric shape, depending on the type and arrangement of rings around it. All the binding energies for the ring positions were found to lie between −0.06 and −0.07 eV, with the exception of the pentagon in the SW defect which produced a slightly lower energy of −0.0727 eV. The 5555-6-7777 defect was the most complex and largest area defect studied, with regions of several unsymmetrical non-hexagonal rings. Yet the fact that its binding value results were similar to that of the smaller area defects suggests that the binding energy in carbon rings is not influenced by the nature of the surrounding rings and the size of the defect area. Hence, it can be speculated that larger and more complex defects that have been discovered or theorized in graphene sheets, consisting of arrangements of rings ranging in size from octagons to pentagons and sp^2 bonded carbon atoms, will likely have binding energies similar to those found for the DV defects in this paper. Binding energies thus seem to be size independent for ring defects.

5.1.3. *Single vacancy defect*

The SV defect on the other hand has quite different characteristics as seen in Fig. 8. Even though the range of charge found to be preferable for binding in ring structures is found around the edges of the vacancy region, the much lower and uneven charge distribution on the carbon atoms adjacent to the vacancy means that the same kind of trend analysis is not applicable. The missing carbon atom in the vacancy leaves behind three dangling bonds on its three adjacent atoms. This causes the defect to undergo a Jahn-Teller distortion which allows two of the adjacent atoms to form a new albeit weak bond between them, replacing two of the dangling bonds. However, one of the dangling bonds remains unable to attach to a second atom and leaves the last adjacent atom with a coordination number of two. As a result, this defect is quite different compared to the other defects studied in this paper, none of which have dangling bonds. The carbon atom with the dangling bond has a dearth of negative electronic charge. This is demonstrated in Fig. 8, which also shows the stronger electron density representing a weak bond between the other two adjacent atoms. This leads to an expectation that the vacancy defect will attract the hydrogen molecule strongly so that it can share in the molecule's cloud of negative charge, making it the preferred adsorption position for the molecule. The dangling bond nature of the SV defect can also be observed by examining PDOS graphs of the defect prior to adsorption and comparing it to that of pristine graphene, as shown in Fig. 11. When the carbon atoms in a ring are able to bond to three adjacent atoms, two of their p_x and p_y orbitals participate in sp^2 hybrid orbitals formed within the plane of the sheet, while the remaining p_z orbitals, oriented

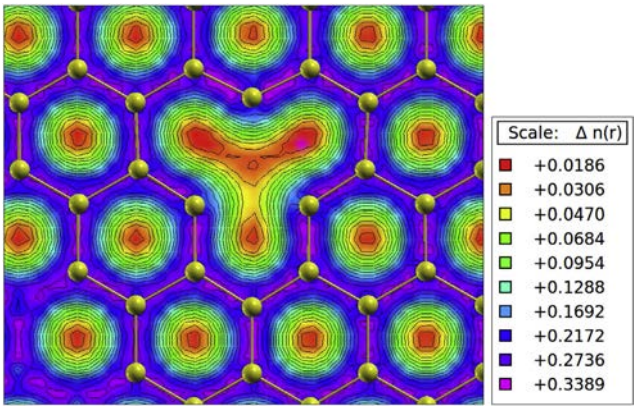

Fig. 8 – Top view charge density plot for the single vacancy defect. The three carbon atoms adjacent to the vacancy can be observed to have lower charge density around them in comparison to the rest of the carbon atoms in the graphene sheet. The carbon atom with a dangling bond is located just above the vacancy in the figure. The other two adjacent atoms have a greater amount of charge between them than the amount of charge between either of them and the dangling bond atom, giving these two adjacent atoms slightly higher stability than the dangling bond atom.

perpendicular to the sheet, overlap and share charge amongst themselves above and below the plane of the sheet. However, when a carbon atom is not able to bond with three other atoms, its p-orbitals are unable to hybridize or overlap to the same extent and are more distinctly localized on the atom as a result. This can be seen in Fig. 11(b), where the greater number of peaks for the p-orbitals indicates more distinct localized states when compared to the much smoother curves for pristine graphene in Fig. 11(a). The unshared charge in these localized orbitals is then more likely to interact with the hydrogen molecule in comparison to charge on more highly co-ordinated atoms in ring structures.

The dangling bond atom would prefer to be close to the hydrogen molecule to share in its increased electronic charge. This could be accomplished by the atom moving out of the plane towards the hydrogen molecule on the side from which the molecule approached or moving in the opposite direction as was observed in our simulation. The first option would cause the dangling bond atom to move further away from its surrounding carbon atoms and give up sharing of charge with them. On the other hand, the latter option allows it to still share in the charge of the graphene sheet while being closer to the hydrogen molecule and is thus the most stable configuration. Fig. 12(a) depicts a side-view of the charge density variation of the vacancy defect. Regular hexagons in pristine graphene, when looked at from the side, have an elongated bright purple region indicating high charge density, as seen at the left and right ends of the figure. On the other hand, the single dangling-bond carbon atom has a smaller circular region of slightly lower and less evenly distributed charge. Furthermore, there is a large gap with moderately low charge between the dangling bond atom and the regular hexagon at the right end of the figure, indicating the electronically deficient vacancy region. Fig. 12(b), shows the cross-sectional charge density after adsorption of the hydrogen molecule. The dangling bond carbon atom possesses a larger region of increased electronic density around the atom. Furthermore, the region between the dangling bond atom and the regular hexagon at the right of the figure and adjacent to the hydrogen molecule clearly shows greatly increased charge density which was probably drawn from the hydrogen molecule.

5.2. *Mixed defect systems*

5.2.1. *Single hydrogen molecule adsorption*

The binding ability of the mixed SW and SV defect was found to be surprisingly strong. Since the two defects individually had the two highest binding energies, mixing them seems to have resulted in an additive effect. Fig. 13(a) shows the charge density plot of this system prior to hydrogen adsorption. The low electron density regions at the single vacancies at the top left and right of the figure (the right vacancy being part of the next repeating unit of the supercell) and the center of the two

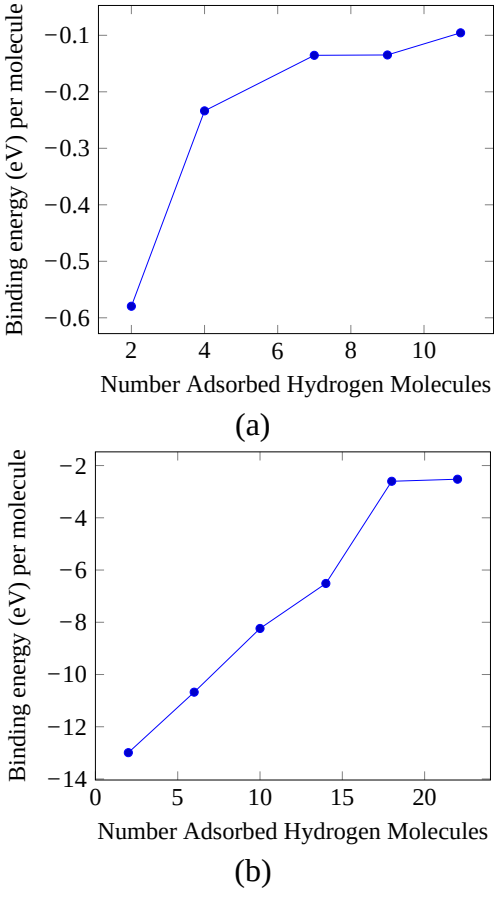

Fig. 9 – Change in average hydrogen binding energy of high defect density systems with increasing number of hydrogen molecules: (a) single vacancy (SVMD) system (b) Stone-Wales and single vacancy (SWSVMD) system.

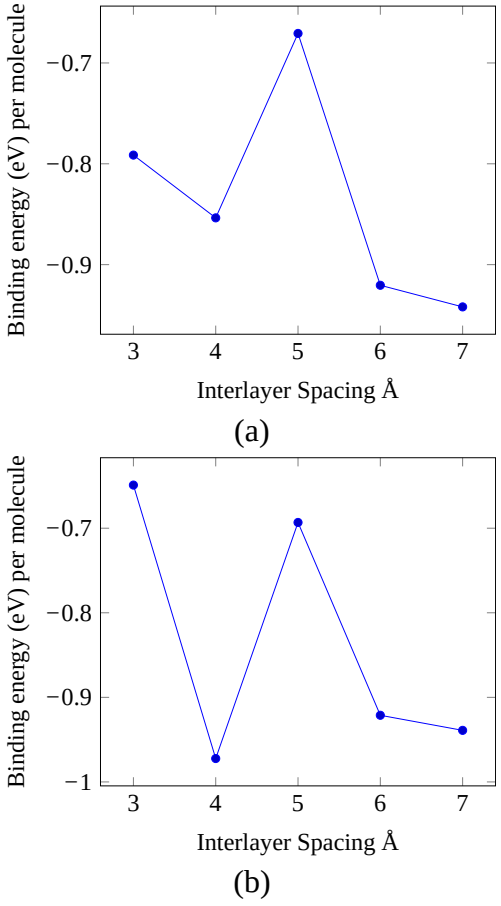

Fig. 10 – The effect of interlayer spacing on the average hydrogen binding energy of high defect density systems: (a) single vacancy (SVMD) system (b) Stone-Wales and single vacancy (SWSVMD) system.

heptagons of the SW defect are clearly visible. The hexagons towards the bottom of the figure have the greatest amount of high charge (purple color) regions while the hexagons towards the top of the figure, between the two vacancies and adjacent to a SW heptagon, have greatly reduced regions of low charge. Presumably some of the charge from the latter hexagons has been transferred to the single vacancies to better stabilize them. Fig. 13(b) shows the charge density plot of the system after hydrogen adsorption. The redistribution of electronic density is now found to be more acute. The region around the pentagon where the hydrogen molecule is adsorbed has significantly lower charge as does the region around the other pentagon towards the bottom of the figure (although to a lesser extent). The single vacancies now show higher charge densities, suggesting that there has been charge transfer from the regions around the pentagons to the single vacancies. The relatively lower charge density around the hydrogen molecule's location would cause it to strongly attract the hydrogen molecule to share in its charge density and would help explain the high hydrogen binding energy for the system. Therefore, the addition of the hydrogen molecule has allowed a greater amount of charge redistribution which has made the single vacancy and hence the entire system more stable.

The results of the mixed SW–SV and grain boundary systems demonstrate that mixed topological defect regions are not detrimental to hydrogen adsorption ability and actually have higher hydrogen binding ability than each isolated individual defect. Yet the mixture of only ring defects, such as that found in the grain boundary system, provide only a modest improvement which is still below levels of desired binding ability. The single vacancy on the other hand seems to greatly enhance the binding ability of ring defects to the required levels. However, its presence is not always beneficial. The reduced binding ability of the nickel atoms when compared with a defect free system might be due to the adjacent vacancy competing with the metal atom for the

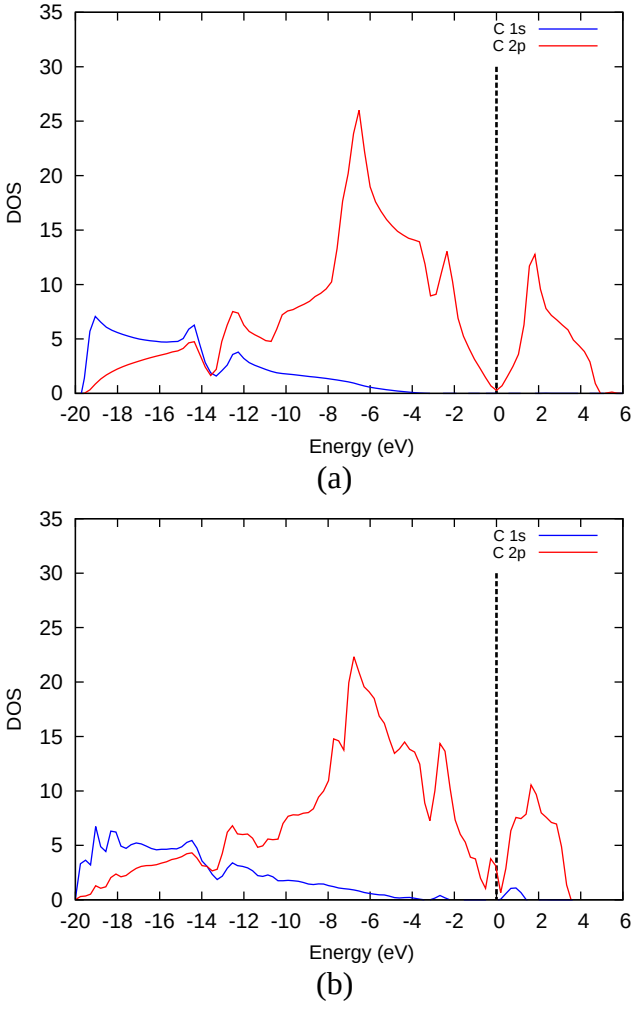

Fig. 11 – Projected Density of States (PDOS) of graphene systems prior to hydrogen adsorption: (a) pristine graphene (b) single vacancy defect (SV). The Fermi level is represented by the dashed vertical line. The dangling bond carbon atom in the SV defect has less co-ordination than atoms in the pristine graphene. Hence, its orbitals have a lower extent of overlap and hybridization, leaving them more distinct and localized. This is visible from the higher number of peaks in the PDOS for the SV defect at all energies. The unshared charge in the more localized SV defect makes it more attractive for adsorbing a hydrogen molecule.

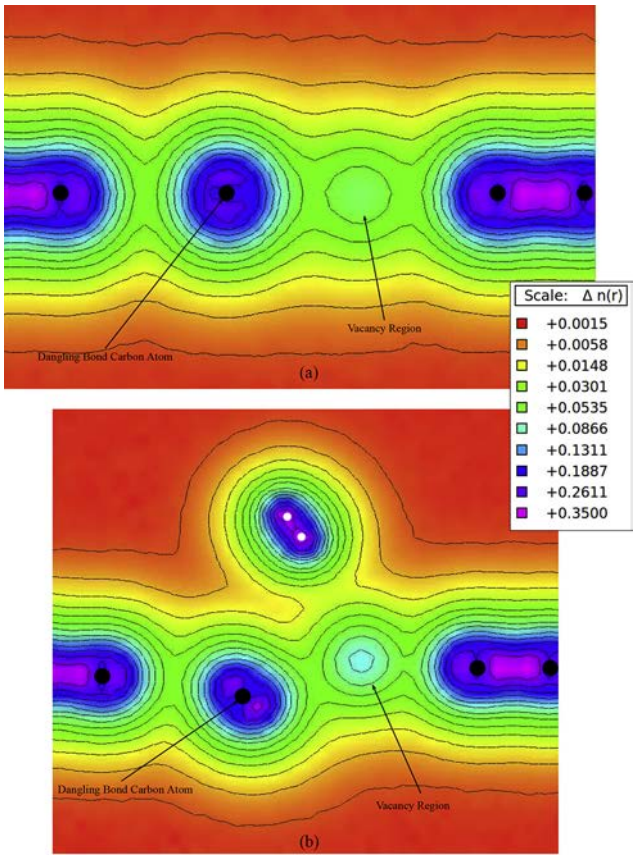

Fig. 12 – Side view of single vacancy (SV) charge density: (a) relaxed SV prior to adsorption and (b) relaxed SV with adsorbed hydrogen molecule. Black filled circles represent carbon atoms, while white filled circles represent hydrogen atoms. Regular hexagons of high charge density usually found in graphene sheets can be seen on the left and right edges of either diagram. In (a), the dangling bond carbon atom has a smaller region of lower charge than the hexagons and the low charge density of the vacancy region is also visible. In (b), the dangling bond carbon atom has higher charge density equivalent to that of the hexagons and the vacancy region also has visibly increased charge density. This increased charge density is likely due to the charge supplied by the hydrogen molecule. (For interpretation of the references to color in this figure legend, the reader is referred to the web version of this article.)

hydrogen molecule's charge and creating a more energetically unfavorable system overall. This indicates that the presence of nearby vacancies might be detrimental to the hydrogen adsorption ability of anchored metal systems. Furthermore, it suggests that it might be more beneficial to construct a structure purely from single vacancies, which provided better binding ability than the investigated nickel adatoms.

5.2.2. *High defect density structures and gravimetric density*
The results of the SVMD and SWSVMD system simulations demonstrate the potential of defect engineered systems for hydrogen storage. The gravimetric density of the SVMD system (5.81%) is just above the initial DOE goal of 5.5%. This is achieved with an average binding energy (−0.1 eV) slightly weaker than the lower limit (−0.2 eV) of binding energy values thought to be required for practical room temperature storage. Therefore, at room temperature conditions, the gravimetric density will likely decrease somewhat to just below target values. The SWSVMD system, on the other hand, has a higher gravimetric density of 7.02%, and its average binding energy (−2.52 eV) is actually much stronger than the higher end (−0.6 eV) of preferred values. With such a strong binding energy, it was surprising that the SWSVMD system was unable to accommodate even more hydrogen molecules. This might possibly be due to crowding of hydrogen molecules and a strong repulsion felt by squeezing additional molecules into the remaining small gaps and destabilizing the carbon–hydrogen complex that had formed. As discussed, these

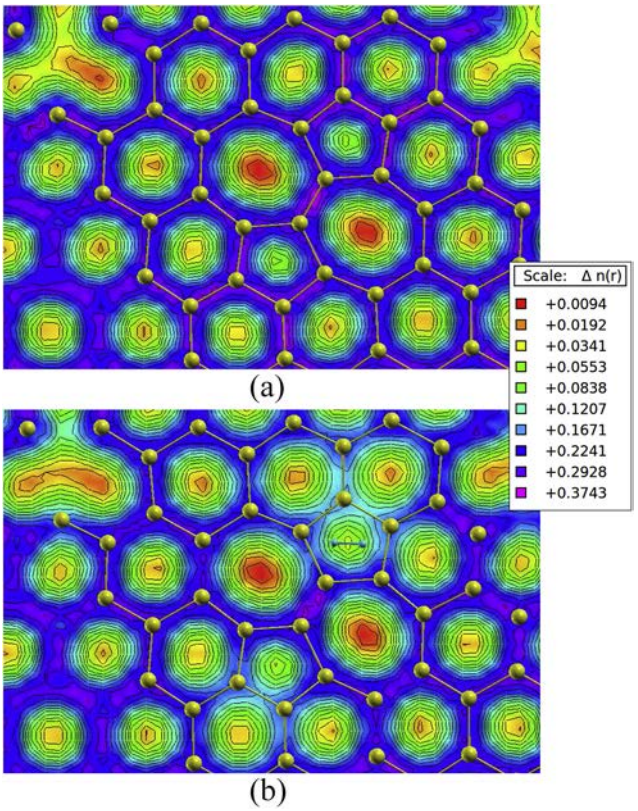

Fig. 13 – Charge density plots of the mixed Stone-Wales and single vacancy system: (a) prior to hydrogen adsorption and (b) subsequent to hydrogen adsorption. Single vacancies are visible at the top left and right of the figures, while the Stone-Wales defect is in the center. There is large redistribution of charge after adsorption of the hydrogen molecule (blue atoms), with the regions around the pentagons of the Stone-Wales defect losing charge to the single vacancies. This lower region of charge then strongly binds the hydrogen molecule, leading to higher hydrogen binding energies than was the case for either defect by itself. (For interpretation of the references to color in this figure legend, the reader is referred to the web version of this article.)

values will likely decrease at room temperature and probably reach desired values.

The designed SVMD and SWSVMD systems thus will likely be able to store hydrogen to a level which is within the ballpark of the DOE targets, with the latter providing higher levels of storage. Yet, they will fall short of the targets in real world conditions as the effects of temperature and fluctuating environmental conditions which cannot be easily modeled become a factor. Furthermore, it is noted here that these results are for the material alone and in a practical storage device with a container and various other components, the hydrogen mass fraction in the whole system will decrease even further. In order to provide a boost in storage ability and a safety factor beyond the targets, additional modifications through the utilization of curvature effects and high pressure environments should allow such defect engineered systems to comfortably meet requirements. This would be achievable without the need for cumbersome and as yet undemonstrated atomic metal decoration.

Clearly interactive effects between graphene layers have played a role in stabilizing the hydrogen atoms, which are mostly located in the voids between successive graphene layers. The change in hydrogen binding energy with interlayer spacing also points to a possible method for reversible storage by controlling interlayer spacing. Certain spacings are more favorable to adsorption and could be used when hydrogen is loaded into and stored in the system. Others are less favorable and likely help cause association and release of hydrogen molecules, which could be used during unloading of hydrogen from the storage system. For instance, for the SVMD system, the interlayer spacing could be changed to 4 Å during unloading to desorb hydrogen and changed to 7 Å during loading to help adsorb hydrogen (although 3 Å provides even stronger binding energy useful for adsorption, it is too close to 4 Å and it might be difficult to maintain a 1 Å gap). For the SWSVMD system, 7 Å would be best for loading and 3 Å would be best for unloading. The control of interlayer spacing through the use of spacer molecules or piezoelectric crystals could be implemented through methods proposed by Tozzini et al. [8]. However, the stability and behavior of the significantly distorted structures during loading and unloading cycles, especially the SWSVMD system which seemed to form a new complex with the hydrogen atoms, might be an issue during practical operation and needs to be further investigated. Nevertheless, mixed defect graphene sheets will undoubtedly prove to be a useful tool in the design and implementation of practical hydrogen storage systems.

6. Conclusion

Commercially prepared low cost graphene is bound to contain topological defects. With significant attention on graphene as a hydrogen storage medium, this paper analyzed the role of topological defects on its hydrogen binding ability and their possible use in defect engineering a better storage system. The ability to adsorb a hydrogen molecule was examined for five types of individual point defects: Stone-Wales, single vacancy and three different double vacancy defects. Two types of density functionals were utilized for all point defect simulations, PBE-GGA and the more recent vdW-DF2 functional which better models long range van der Waals forces. The vdW-DF2 simulations in general resulted in a stronger hydrogen binding ability than PBE-GGA, demonstrating that the vdW forces are a significant factor in hydrogen molecule adsorption and should be accounted for to accurately model this phenomenon. The vdW-DF2 results also showed a smaller variation in binding energies for different H_2 binding sites than the PBE-GGA computations. The single vacancy defect had the strongest binding value and had the only value which fell within the range desirable for reversible hydrogen adsorption. The Stone-Wales and double vacancy defects did not display significant improvement in binding ability over that of pristine graphene, however they were shown to not have a detrimental effect on hydrogen storage ability. Defects consisting of various planar carbon rings ranging in size from pentagons to octagons, such as the Stone-Wales and double vacancy defects, were found to have similar hydrogen binding values and the binding value for a particular site within such a ring was found to be independent of the nature of the surrounding rings or defect size range.

Subsequent to investigation of isolated defects, a number of multiple defect systems were modeled using the vdW-DF2 functional only. A grain boundary system analogous to a Σ7 grain boundary defect and consisting of pentagon and heptagon rings was found to have a hydrogen binding energy similar to that of the Stone-Wales and double vacancy ring defects. A metal decorated system, consisting of vacancy anchored nickel adatoms with an adjacent undecorated vacancy, was simulated and it was found that the presence of an undecorated vacancy decreased the binding ability of the nickel adatom when compared to a system with no vacancies. On the other hand, the presence of a single vacancy was found to significantly enhance the hydrogen binding ability of an adjacent Stone-Wales defect and move its hydrogen binding energy into the range desirable for reversible hydrogen adsorption. Two high defect density systems, the first consisting of only closely spaced single vacancies and the second consisting of closely spaced single vacancies and Stone-Wales defects, were then designed and tested for their ability to bind a large number of hydrogen molecules. The first system managed to produce a maximum gravimetric density of 5.81% while the latter achieved 7.02%. These results were achieved at relatively small graphene interlayer spacings, with both systems showing the best average hydrogen binding energy at 3 Å spacing and weaker binding ability for both smaller and larger spacings. Hence, defect engineering of graphene systems shows great potential in meeting hydrogen storage requirements while avoiding the need for the potentially more challenging metal decoration that is proposed currently.

Acknowledgments

The authors gratefully acknowledge financial support from the Natural Sciences and Engineering Research Council

(NSERC) and the University of Toronto. Computations were performed on the HPC supercomputer at the SciNet HPC Consortium [32] and Calcul Quebec/Compute Canada. SciNet is funded by: the Canada Foundation for Innovation under the auspices of Compute Canada; the Government of Ontario; Ontario Research Fund – Research Excellence; and the University of Toronto.

REFERENCES

[1] Lim KL, Kazemian H, Yaakob Z, Daud WRW. Solid-state materials and methods for hydrogen storage: a critical review. Chem Eng Technol 2010 Feb;33(2):213–26.
[2] Targets for onboard hydrogen storage systems for light-duty vehicles. US Department of Energy Office of Energy Efficiency and Renewable Energy and The FreedomCAR and Fuel Partnership; 2009.
[3] Firlej L, Kuchta B, Wexler C, Pfeifer P. Boron substituted graphene: energy landscape for hydrogen adsorption. Adsorption 2009;15:312–7.
[4] Jena P. Materials for hydrogen storage: past, present, and future. J Phys Chem Lett 2011 Feb;2(3):206–11.
[5] Sun Y, Wu Q, Shi G. Graphene based new energy materials. Energy Environ Sci 2011;4:1113–32.
[6] Yoon M, Yang S, Wang E, Zhang Z. Charged fullerenes as high-capacity hydrogen storage Media. Nano Lett 2007;7(9):2578–83.
[7] Henwood D, Carey J. Ab initio investigation of molecular hydrogen physisorption on graphene and carbon nanotubes. Phys Rev B 2007 Jun;75(24):245413.
[8] Tozzini V, Pellegrini V. Prospects for hydrogen storage in graphene. Phys Chem Chem Phys PCCP 2013 Jan;15(1):80–9.
[9] Wang V, Mizuseki H, He HP, Chen G, Zhang SL, Kawazoe Y. Calcium-decorated graphene for hydrogen storage: a van der Waals density functional study. Comput Mater Sci 2012 Apr;55:180–5.
[10] Singh AK, Yakobson BI. First principles calculations of H-storage in sorption materials. J Mater Sci 2012 May;47(21):7356–66.
[11] Wang L, Lee K, Sun YY, Lucking M, Chen Z, Zhao JJ, et al. Graphene oxide as an ideal substrate for hydrogen storage. ACS nano 2009 Oct;3(10):2995–3000.
[12] Pumera M. Graphene-based nanomaterials for energy storage. Energy & Environ Sci 2011;4(3):668.
[13] Banhart F, Kotakoski J, Krasheninnikov AV. Structural defects in graphene. ACS nano 2011 Jan;5(1):26–41.
[14] Bhattacharya A, Bhattacharya S, Majumder C, Das GP. Transition-metal decoration enhanced room-temperature hydrogen storage in a defect-modulated graphene sheet. J Phys Chem C 2010;114(22):10297–301.
[15] Robertson AW, Allen CS, Ya Wu, He K, Olivier J, Neethling J, et al. Spatial control of defect creation in graphene at the nanoscale. Nat Commun 2012 Jan;3:1144.
[16] Lee K, Murray ED, Kong L, Lundqvist BI, Langreth DC. Higher-accuracy van der Waals density functional. Phys Rev B 2010 Aug;82(8):081101.
[17] Giannozzi P, Baroni S, Bonini N, Calandra M, Car R, Cavazzoni C, et al. QUANTUM ESPRESSO: a modular and open-source software project for quantum simulations of materials. J Phys Condens Matter 2009;21:395502.
[18] Perdew JP, Burke K, Ernzerhof M. Generalized gradient approximation made simple. Phys Rev Lett 1996;77(18):3865–8.
[19] Vanderbilt D. Soft self-consistent pseudopotentials in a generalized eigenvalue formalism. Phys Rev B 1990;41(11):7892.
[20] Monkhorst HJ, Pack JD. Special points for brillouin-zone integrations. Phys Rev B 1976;13(12):5188–92.
[21] Methfessel M, Paxton AT. High-precision sampling for brillouin-zone integration in metals. Phys Rev B 1989 Aug;40:3616–21.
[22] Dion M, Rydberg H, Schröder E, Langreth DC, Lundqvist BI. Van der Waals density functional for general geometries. Phys Rev Lett 2004 Jun;92(24):246401.
[23] Lee K, Berland K, Yoon M, Andersson S, Schröder E, Hyldgaard P, et al. Benchmarking van der Waals density functionals with experimental data: potential-energy curves for H2 molecules on Cu(111), (100) and (110) surfaces. J Phys Condens Matter: Inst Phys J 2012 Oct;24(42):424213.
[24] Li G, Tamblyn I, Cooper VR, Gao HJ, Neaton JB. Molecular adsorption on metal surfaces with van der Waals density functionals. Phys Rev B 2012 Mar;85:121409.
[25] Kokalj A. Computer graphics and graphical user interfaces as tools in simulations of matter at the atomic scale. Comput Mater Sci 2003;28(2):155–68. Proceedings of the Symposium on Software Development for Process and Materials Design.
[26] Costanzo F, Silvestrelli PL, Ancilotto F. Physisorption, diffusion, and chemisorption pathways of H(2) molecule on graphene and on (2,2) carbon nanotube by first principles calculations. J Chem Theory Comput 2012;8(4):1288–94. ST – Physisorption, Diffusion, and Chem.
[27] Young-Kyun K. Hydrogen adsorption on sp^2-bonded carbon structures: ab-initio study. J Korean Phys Soc 2010 Oct;57(4):778.
[28] Zhang J, Zhao J, Lu J. Intrinsic strength and failure behaviors of graphene grain boundaries. ACS Nano 2012;6(3):2704–11.
[29] Wong J, Tam J, Yadav S, Singh CV. A van der Waals DFT comparison of metal decorated graphene systems for hydrogen adsorption. Unpublished;.
[30] Kim G, Jhi SH, Lim S, Park N. Effect of vacancy defects in graphene on metal anchoring and hydrogen adsorption. Appl Phys Lett 2009;94(17):173102.
[31] Chen L, Hu H, Ouyang Y, Pan HZ, Sun YY, Liu F. Atomic chemisorption on graphene with StoneThrowerWales defects. Carbon 2011;49(10):3356–61.
[32] Loken C, Gruner D, Groer L, Peltier R, Bunn N, Craig M, et al. SciNet: lessons learned from building a power-efficient top-20 system and data centre. J Phy Conf Ser 2010;256:012026.